Journal of Solid State Chemistry 183 (2010) 557–564

Contents lists available at ScienceDirect

Journal of Solid State Chemistry

journal homepage: www.elsevier.com/locate/jssc

The crystal structures of $Hf_{3\pm\delta}Nb_{4\pm\delta}As_3$ and $Hf_{7.2}Nb_{3.8}As_4$: Members of a homologous series combining W-type, Mg-type and AlB_2-type building blocks

Igor Chumak [1], Piotr Warczok, Klaus W. Richter *

Department of Inorganic Chemistry/Materials Chemistry, University of Vienna, Waehringerstr. 42, A-1090 Wien, Austria

ARTICLE INFO

Article history:
Received 7 October 2009
Received in revised form
17 December 2009
Accepted 29 December 2009
Available online 6 January 2010

Keywords:
As–Hf–Nb system
Transition metal arsenides
Crystal structure
Partial ordering

ABSTRACT

Two new partially ordered compounds were synthesized in the system Hf–Nb–As by arc melting and subsequent annealing at 1400 °C and they were structurally characterized by means of single crystal X-ray diffraction. The compound $Hf_{3\pm\delta}Nb_{4\pm\delta}As_3$ is isostructural to $Zr_3Pd_4P_3$ and $Hf_3Pd_4P_3$ (Space group: *Pnma*, Pearson symbol *oP*40) and shows a considerable homogeneity range between the limiting compositions $Hf_{2.4}Nb_{4.6}As_3$ and $Hf_{4.1}Nb_{2.9}As_3$. Mixed occupation of Hf and Nb were found at all seven independent metal sites, with varying Hf/Nb ratios, so the compound is stabilized by differential fractional site occupation (DFSO). The compound $Hf_{7.2}Nb_{3.8}As_4$ is isostructural with $Zr_{6.45}Nb_{4.55}P_4$ (*Immm*, *oI*30) and was found to be metastable at the temperature of annealing (1400 °C). Similar to the type structure, $Hf_{7.2}Nb_{3.8}As_4$ is stabilized by (DFSO). Structural relations of the two compounds with $Hf_{1.5+\delta}Nb_{1.5-\delta}As$ (*Pnma*, *oP*16) are discussed. All three compounds belong to a homologous series $M_{k+2l+m}X_{2m}$ combining W-type, Mg-type and AlB_2-type building blocks.

1. Introduction

A great variety of pnictides of the early transition metals have been synthesized in the past decades. While the metal-poor compounds (*MX* and MX_2) are structurally simple, metal-rich phosphides, arsenides and antimonides are showing a rich structural chemistry with variety of different structure types and stoichiometries. A common feature found in many of these metal-rich compounds is the existence of building blocks that resemble the bcc-structure (W-type) of the pure transition metals. These building blocks are part of an extended metal framework and are usually interconnected by pnictide-centred trigonal-prismatic units.

A variety of new ternary compounds $(M,M')_xX_y$ with similar structural features were synthesized in recent years by the application of the concept of differential fractional site occupation (DFSO) [1]. In DFSO-stabilized compounds, random mixtures of the two closely related metals *M* and *M*′ are found at the different metal sites, but the ratio *M*/*M*′ varies from site to site (substitutional partial ordering). A review on DFSO-stabilized pnictides and chalcogenides was given by Kleinke [2]. More recent examples include the ternary arsenides $(Ti,Mo)_5As_3$ with Yb_5Bi_3-type structure (*Pnma*) [3], Ti_2MoAs_2 (V_3As_2-type, *P*4/*m*) and Ti_3MoAs_3 (Cr_4As_3-type, *C*2/*m*) [4]. In an ongoing research project, we systematically investigated partial ordering in *M*–*M*′–Ge systems and synthesized several new ternary compounds and solid solutions stabilized by differential fractional site occupation in the systems Ta–Zr–Ge [5,6], Hf–Nb–Ge [7], Hf–Zr–Ge [8] and Zr–V–Ge [9]. One of our main goal in this investigation was the rationalization of the site preferences observed in these compounds. The different approaches used to understand the varying metal ratios at crystallographically different sites include basic size considerations (using the volume of the Wigner–Seitz cell as measure for the space available at a specific site) and various bonding arguments based on electronic calculations [10]. We also successfully employed ground state energies obtained by DFT calculations for thermodynamic modelling of partial ordering in these compounds [8,11].

Recently, we extended these investigations also to the system Hf–Nb–As and reported on the two new DFSO stabilized compounds $Hf_{1.5+\delta}Nb_{1.5-\delta}As$ (own type, *Pnma*) and $Hf_{2+\delta}Nb_{1-\delta}As$ (Ti_3P-type, $P4_2/n$) [12] and the distribution of Hf and Nb over the respective metal sites could be excellently described by the combination of DFT ground state energies with thermodynamic models. In the current work, we report on the synthesis and structural characterization of two additional DFSO-stabilized ternary compounds in the Hf–Nb–As system and discuss their common structural features.

2. Methods

The samples were prepared from Hf powder (Alfa Aesar, containing 2–3.5% Zr, content of Hf+Zr metal basis 99.6%), Nb powder (Alfa Aesar with a content of Ta < 500 ppm, content of Nb+Ta metal basis 99.99%) and As polycrystalline lumps (Johnson

* Corresponding author. Fax: +431 4277 9529.
E-mail address: klaus.richter@univie.ac.at (K.W. Richter).
[1] Present address: IWF Dresden, Institut für Komplexe Materialien, Helmholtzstr. 20, 01069 Dresden, Germany.

0022-4596/$ - see front matter © 2010 Elsevier Inc. All rights reserved.
doi:10.1016/j.jssc.2009.12.028

Matthey, 99.9999%). The materials were stored and handled in the glove-box in order to avoid a longer exposure to air. Before use, the arsenic lumps were heated in a silica tube under dynamic vacuum, in order to remove any arsenic oxides from the surface.

Due to the high vapour pressure of As, the samples were prepared in two steps. The monoarsenides HfAs and NbAs were prepared as master alloys from the pure elements in evacuated silica tubes. The powder mixture was heated to 900 °C within 2 days, and then annealed at this temperature for 3 days. Calculated amounts of the master alloys and pure metal powders were weighed to a sample mass of 1000 mg. The powders were mixed and pressed to pellets with a diameter of 5 mm which were subsequently melted in the arc-furnace under an argon atmosphere and the mass losses due to As-evaporization (in the order of 3–30 mg, depending on the starting composition) were routinely checked after arc melting. The arc melted samples were finally sealed in closed tantalum crucibles under 0.5 bar Ar, annealed at 1400 °C for 3 days and quenched in a water-cooled steel vessel under argon.

Table 1
Crystal data and structure refinements for $Hf_{3\pm\delta}Nb_{4\pm\delta}As_3$ ($Hf_{3.3}Nb_{3.7}As_3$) and $Hf_{7.2}Nb_{3.8}As_4$.

Empirical formula	$Hf_{3.3}Nb_{3.7}As_3$	$Hf_{7.2}Nb_{3.8}As_4$
Unit cell dimensions	a=17.964(3) Å	a=3.5825(7) Å
	b=3.5869(7) Å	b=9.6162(19) Å
	c=11.262(2) Å	c=16.103(3) Å
	V=725.7(2) Å^3	V=554.74(19) Å^3
Crystal system, space group	Orthorhombic, *Pnma*	Orthorhombic, *Immm*
Structure type	$M_3Pd_4P_3$ (M=Zr, Hf)	$Zr_{6.45}Nb_{4.55}P_4$
Z	4	2
Calculated density	10.601 g/cm^3	11.691 g/cm^3
Absorption coefficient	66.185 mm^{-1}	84.021 mm^{-1}
Crystal dimensions	60 × 60 × 30 μm	50 × 40 × 40 μm
Range of data collection	$5.8 < 2\vartheta < 50.0°$	$8.5 < 2\vartheta < 60.2°$
Scan mode (at distinct ω-angles)	φ-scans	φ-scans
Reflections collected/unique	4380/752	2580/508
Number of refined parameters	69	33
GooF = $\{\sum[w(F_o^2-F_c^2)^2]/(n-p)\}^{1/2}$	1.092	1.189
$R1 = \sum(\|\|F_o\|-\|F_c\|\|)/\sum F_o$	0.0501	0.0260
wR2 = $[\sum w(F_o^2-F_c^2)^2/\sum\|wF_o^4\|]^{1/2}$	0.1253	0.0628
Extinction coefficient	–	0.00043(6)
Final difference Fourier map (eÅ^{-3})	5.098 to −4.912 eÅ^{-3}	3.734 to −3.281

Initial sample characterization was performed by X-ray powder diffraction using a Bruker AXS D8 powder diffractometer in Bragg–Brentano reflection setting and Cu$K\alpha$-radiation using a high-speed 1-dimensional Si-strip detector (Lynxeye). Phase identification and pattern refinement were performed with the Topas Software [13] applying the fundamental parameter approach for peak profile modelling.

Pieces of the annealed samples were embedded in resin, ground and polished for metallographic investigation by optical light microscopy and scanning electron microscopy. The phase compositions were analysed by EPMA on a Cameca SX electron probe 100 using wavelength dispersive spectroscopy (WDS) for quantitative analyses and employing pure hafnium, niobium and GaAs as standard materials. The measurements were carried out at 20 kV and a beam current of 20 nA using the Hf$M\alpha$, Nb$L\alpha$ and As$L\beta$ emission lines for intensity measurements. Conventional ZAF matrix correction was used to calculate the final compositions from the measured X-ray intensities.

The single crystals for structure determination were separated from the bulk sample under an optical microscope. Diffraction data were collected on a Bruker SMART CCD diffractometer equipped with a CCD detector and a 300 μm capillary-optics collimator (Mo tube, graphite monochromator). The unit cell parameters were obtained by least-squares refinements of 2ϑ values. Corrections for Lorentz, polarization and absorption effects were done by application of the multi-scan method [14]. The structure solution by direct methods and subsequent structure refinement was performed using the Shelx97 software package [15]. Selected information on single crystal X-ray data collection and refinements is given in Table 1 and the structural parameters of the two title compounds are compiled in Table 2. Further details of the crystal structure investigations can be obtained from the Fachinformationszentrum Karlsruhe, 76344 Eggenstein-Leopoldshafen, Germany, (Fax: +49 7247 808 666; e-mail: crysdata@fiz.karlsruhe.de) on quoting the depository numbers CSD 421068 and 421069.

3. Results and discussion

3.1. $Hf_{3\pm\delta}Nb_{4\pm\delta}As_3$

The compound $Hf_{3\pm\delta}Nb_{4\pm\delta}As_3$ was found in eight samples with different compositions in the metal-rich part of the ternary Hf–Nb–As system. These samples contained $Hf_{3\pm\delta}Nb_{4\pm\delta}As_3$ in equilibrium with various binary and ternary phases. An investigation of the

Table 2
Atomic coordinates and equivalent displacement parameters for $Hf_{3\pm\delta}Nb_{4\pm\delta}As_3$ ($Hf_{3.3}Nb_{3.7}As_3$) and $Hf_{7.2}Nb_{3.8}As_4$.

Site	Wyckoff position	x	y	z	$U(eq)$ (Å$^2\times10^3$)	Occupation
$Hf_{3\pm\delta}Nb_{4\pm\delta}As_3$; Pnma						
*M*1	4*c*	0.0874(1)	1/4	0.6811(2)	10(1)	0.12(1) Hf+0.88(1) Nb
*M*2	4*c*	0.1312(1)	1/4	0.1095(2)	10(1)	0.21(1) Hf+0.79(1) Nb
*M*3	4*c*	0.2395(1)	1/4	0.5026(1)	11(1)	0.91(1) Hf+0.09(1) Nb
*M*4	4*c*	0.2926(1)	1/4	0.2206(2)	11(1)	0.15(1) Hf+0.85(1) Nb
*M*5	4*c*	0.3235(1)	1/4	0.7944(2)	11(1)	0.20(1) Hf+0.80(1) Nb
*M*6	4*c*	0.4407(1)	1/4	0.4160(1)	11(1)	0.85(1) Hf+0.15(1) Nb
*M*7	4*c*	0.0410(1)	1/4	0.3839(1)	11(1)	0.87(1) Hf+0.13(1) Nb
*As*1	4*c*	0.1745(2)	1/4	0.8818(2)	10(1)	1.00 As
*As*2	4*c*	0.3794(2)	1/4	0.0178(2)	10(1)	1.00 As
*As*3	4*c*	0.4629(2)	1/4	0.6891(2)	11(1)	1.00 As
$Hf_{7.2}Nb_{3.8}As_4$; Immm						
*M*1	8*l*	0	0.1559(1)	0.2908(1)	7(1)	0.32(1) Hf+0.68(1) Nb
*M*2	4*j*	1/2	0	0.1603(1)	8(1)	1.00(1) Hf
*M*3	4*j*	1/2	0	0.4035(1)	10(1)	0.66(1) Hf+0.34(1) Nb
*M*4	4*h*	0	0.2184(1)	1/2	9(1)	0.97(1) Hf+0.03(1) Nb
*M*5	2*a*	0	0	0	7(1)	0.69(1) Hf+0.31(1) Nb
As	8*l*	0	0.2060(1)	0.1198(1)	4(1)	1.00 As

complex phase equilibria in Hf–Nb–As at 1400 °C is currently in progress and will be published separately. A single crystal suitable for structure determination was picked from a sample with the nominal overall composition 26.9 at% Hf, 53.5 at% Nb, 19.6 at% As which contained $Hf_{3\pm\delta}Nb_{4\pm\delta}As_3$ in equilibrium with a solid solution of metallic Nb and Hf (W-type). The eight samples containing $Hf_{3\pm\delta}Nb_{4\pm\delta}As_3$ in equilibrium with various binary and ternary phases were investigated by powder XRD and EPMA in order to determine the exact composition range of the compound. EPMA measurements revealed that $Hf_{3\pm\delta}Nb_{4\pm\delta}As_3$ exhibits a considerable homogeneity range from approximately 29 to 46 at% Nb. The lattice parameters vary from a=17.740(1) Å, b=3.5553(1) Å, c=11.1130(3) Å for $Hf_{2.4}Nb_{4.6}As_3$ (Hf-poor composition limit) to a=17.997(1) Å, b=3.5916(1) Å, c=11.2910(3) Å for $Hf_{4.1}Nb_{2.9}As_3$ (Hf-rich composition limit). The experimental lattice parameters and the phase composition of $Hf_{3\pm\delta}Nb_{4\pm\delta}As_3$ determined by EPMA are summarized in Table 3. The annealed samples were generally well homogenized and the course of lattice parameters with the composition show a clear trend but noticeable scattering. The increase of lattice parameters with the Hf-content is in good agreement with the larger atomic radius of Hf compared to Nb (Pauling radii: Hf 144 pm, Nb 134 pm [16]). In contrast to the significant variability of the Hf/Nb ratio, the As-content of the phase was found to be 30 at% in all samples without any variation.

$Hf_{3\pm\delta}Nb_{4\pm\delta}As_3$ was found to be isostructural to the compounds $M_3Pd_4P_3$ (M=Zr, Hf) [17]. Atomic coordinates listed in Table 2 reveal that all 10 sites (seven metal sites and three arsenic sites) are situated at 4c positions, site symmetry m, i.e. within the mirror plane at y=1/4 and 3/4 and the structure is correspondingly characterized by a short b-axis. As expected, Hf and Nb are not evenly distributed over the seven metal sites, but show strong site preferences. The single crystal used for structure determination has the refined composition $Hf_{3.3}Nb_{3.7}As_3$, and is thus situated more or less in the incentre of the homogeneity range. All seven metal positions show mixed site occupation with varying Hf/Nb ratios; however, two distinctively different sets of sites can be determined based on the occupation factors. While three of the seven metal sites, M3, M6 and M7, show Hf-rich site fractions with occupation numbers between 0.85 and 0.91 Hf, the other four sites, M1, M2, M4 and M5 are occupied by Nb-rich Hf/Nb mixtures with Hf-occupation ranging between 0.21 and 0.12. Thus, site preferences in this compound are massive, indicating a strong stabilizing effect of preferred site occupation, i.e. significant energies of substitution. The selected phase designation, $Hf_{3\pm\delta}Nb_{4\pm\delta}As_3$, reflects these site preferences with three Hf-rich and four Nb-rich metal positions, i.e. a situation similar to the completely ordered type compounds $M_3Pd_4P_3$ (M=Zr, Hf). However, unlike to these compounds, our experimental data clearly show that a completely ordered compound at the composition $Hf_3Nb_4As_3$ does not exist, as $Hf_{3.3}Nb_{3.7}As_3$ (i.e. at a lower Nb-content) already shows the presence of Nb at all seven metal positions. As it was not possible to isolate additional single crystals with other phase compositions, the change of occupation factors with the composition cannot be given in detail. However, we assume that the occupation numbers of the two different sets of sites, (M3, M6, M7) and (M1, M2, M4, M5), will change with the composition in a more or less simultaneous way.

A projection of the crystal structure of $Hf_{3\pm\delta}Nb_{4\pm\delta}As_3$ along the short b-axis is shown in Fig. 1. All three As-sites are coordinated by tri-capped trigonal prisms of metal atoms (CN=9) stacked in the direction of the short b-axis. The basal planes of these trigonal prismatic units are shown as grey triangles in Fig. 1. One of the metal sites, M5, is situated in the centre of a distorted bcc-like fragment with distances to the eight neighbouring M-atoms ranging from 2.86 to 3.19 Å, which corresponds well to the M–M distance in bcc-type Nb (2.87 Å) and Hf (3.13 Å). The coordination spheres of M1, M2 and M4 also resemble the bcc structure with a total coordination number of 14, i.e. 8+6 in the first and second coordination sphere, respectively, but the distorted cube forming the first coordination sphere contains 6 M- and 2 As-positions. M3, M6 and M7 (these are the nodes connecting the trigonal prismatic units) are showing a significantly different coordination, i.e. capped pentagonal prisms with a total coordination number of 17. The coordination polyhedra of all seven metal positions of $Hf_{3\pm\delta}Nb_{4\pm\delta}As_3$ are shown in Fig. 2. The existence of two significantly different sets of coordination

Table 3
Phase compositions and lattice parameters of $Hf_{4-\delta}Nb_{3+\delta}As_3$ in different samples.

Nominal sample composition (at% Hf, at% Nb, at% As)	Lattice parameters (Å)	Phase composition of $Hf_{4-\delta}Nb_{3+\delta}As_3$ by EPMA (at% Hf, at% Nb, at% As)
21.9, 49.0, 29.1	a=17.740(1), b=3.5553(1), c=11.1130(3)	23.8, 46.2, 30.0
14.6, 58.0, 27.4	a=17.736(1), b=3.5571(1), c=11.1136(2)	Not determined due to fine microstructure
28.6, 42.6, 28.8	a=17.910(1), b=3.5779(1), c=11.1979(3)	27.0, 43.0, 30.0
35.8, 35.5, 28.6	a=17.853(1), b=3.5725(1), c=11.1653(4)	28.3, 41.7, 30.0
26.9, 53.5, 19.6	a=17.925(1), b=3.5785(1), c=11.2027(4)	28.7, 41.3, 30.0
30.3, 49.9, 19.8	a=17.930(1), b=3.5790(1), c=11.2235(4)	31.4, 38.7, 29.9
41.9, 37.1, 21.0	a=17.966(1), b=3.5875(1), c=11.2532(3)	39.5, 30.6, 29.9
42.6, 28.6, 28.7	a=17.997(1), b=3.5916(1), c=11.2910(3)	40.8, 29.3, 29.9

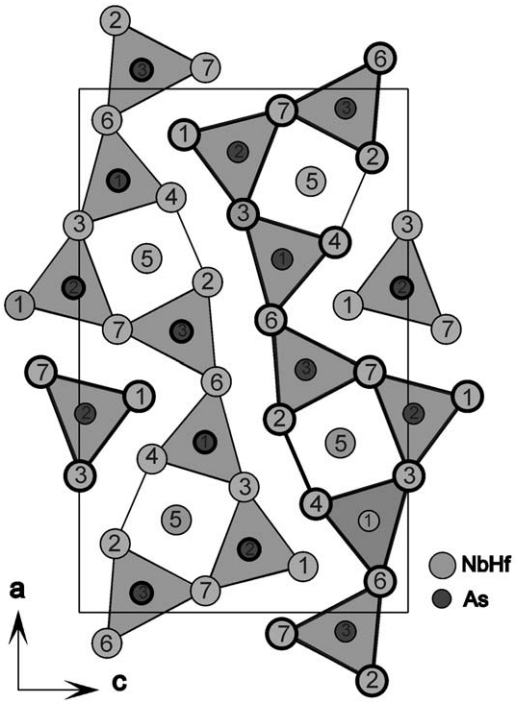

Fig. 1. The crystal structure of $Hf_{3\pm\delta}Nb_{4\pm\delta}As_3$ (Space group: *Pnma*, Pearson symbol: *oP*40) projected in [010] direction. Grey triangles: trigonal prismatic units centred by As. As and M-sites are numbered according to the site designation given in Table 2. The M-atoms at y=0.75 are connected with thick lines, at y=0.25 with thin lines.

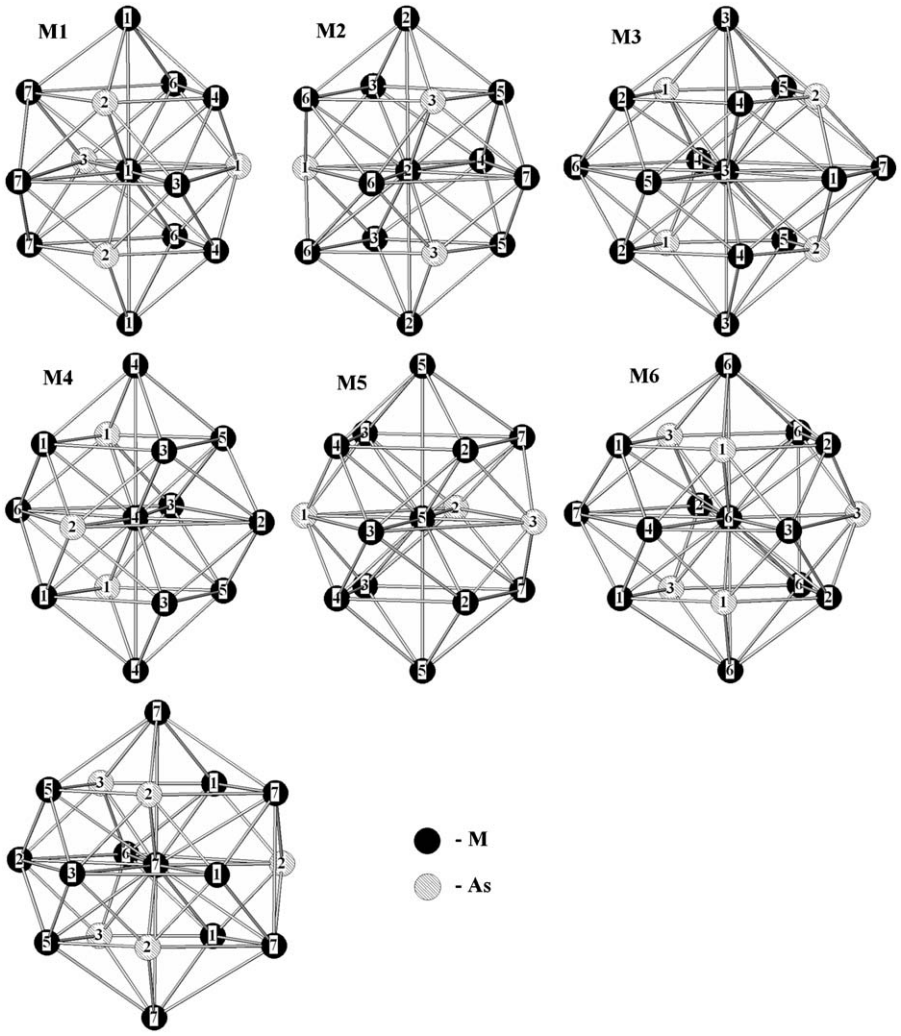

Fig. 2. Coordination polyhedra of the seven independent metal sites in $Hf_{3\pm\delta}Nb_{4\pm\delta}As_3$. The numbers correspond to the numbering of sites in Table 2.

Table 4
Volume of the Wigner–Seitz cell and cumulated Pauling bond orders (PBOs) of the metal positions in $Hf_{3\pm\delta}Nb_{4\pm\delta}As_3$ ($Hf_{3.3}Nb_{3.7}As_3$) and $Hf_{7.2}Nb_3.8As_4$.

$Hf_{3\pm\delta}Nb_{4\pm\delta}As_3$		$Hf_{7.2}Nb_{3.8}As_4$			
Site	Site volume (Å^3)	Site	Site volume (Å^3)	Total PBO	*M*–*M* PBO
*M*1	17.86	*M*1	18.27	5.44	3.48
*M*2	18.63	*M*2	19.59	4.95	2.21
*M*3	19.59	*M*3	20.43	4.40	3.60
*M*4	17.69	*M*4	19.91	4.87	1.97
*M*5	18.78	*M*5	20.01	4.55	2.26
*M*6	19.94				
*M*7	20.04				

environments for the metal positions provides a good explanation for the strong site preferences observed in this compound. Thus, Nb preferably occupies the less coordinated positions *M*1, *M*2, *M*4 and *M*5 while the higher coordinated positions *M*3, *M*6 and *M*7 are preferably occupied by Hf. An analysis of the site volumes leads to the same conclusions, as *M*3, *M*6 and *M*7 show significantly larger site volumes than *M*1, *M*2, *M*4 and *M*5. The corresponding volumes of the Wigner–Seitz cells calculated using the programme DIDO [18] are given in Table 4. Selected interatomic distances in $Hf_{3\pm\delta}Nb_{4\pm\delta}As_3$ are given in Table 5.

3.2. $Hf_{7.2}Nb_{3.8}As_4$

A crystal of the compound $Hf_{7.2}Nb_{3.8}As_4$ was picked from the surface of a sample with the nominal composition 40.2 at% Hf, 39.9 at% Nb and 19.9 at% As. Structure solution and refinement as compiled in Tables 1 and 2 revealed an orthorhombic structure, space group *Immm*, Pearson symbol *oI*30 which was found to be isostructural with $Zr_{6.45}Nb_{4.55}P_4$ [19]. The X-ray powder diffractogram of the sample from which the crystal was isolated did not show the lines corresponding to $Hf_{7.2}Nb_{3.8}As_4$, nor could this pattern be observed in any of the other samples investigated. It is therefore concluded that $Hf_{7.2}Nb_{3.8}As_4$ is only metastable at the temperature of annealing (1400 °C).

Structural features of the $Zr_{6.45}Nb_{4.55}P_4$ have already been discussed by Marking and Franzen [19] and a graphical representation of the crystal structure projected along the short *a*-axis is given in Fig. 3. Please note that the selection of axis and numbering of atomic positions used in this work differs from the setting used in [19] as the structure data used in the current work were transformed to the standard setting using the programme *Structure Tidy* [20]. Similar to the coordination polyhedra found in $Hf_{3\pm\delta}Nb_{4\pm\delta}As_3$, three different groups of coordination environments can be identified. The *As* site shows a tri-capped trigonal primatic coordination (CN=9), while the metal atoms show two different coordination environments with

Table 5
Selected interatomic distances in $Hf_{3\pm\delta}Nb_{4\pm\delta}As_3$ ($Hf_{3.3}Nb_{3.7}As_3$).

Bond		Distance (Å)	Bond		Distance (Å)	Bond		Distance (Å)
*As*1	*M*4	2.619(3) (2 ×)	*M*2	*As*3	2.622(3) (2 ×)	*M*6	*As*3	2.760(2) (2 ×)
	*M*2	2.681(3)		*As*1	2.681(3)		*As*1	2.766(3) (2 ×)
	*M*3	2.730(2) (2 ×)		*M*5	2.866(2) (2 ×)		*As*3	3.102(3)
	*M*1	2.749(4)		*M*6	3.104(2) (2 ×)		*M*2	3.104(2) (2 ×)
	*M*6	2.766(3) (2 ×)		*M*4	3.158(3)		*M*1	3.235(2) (2 ×)
	*M*5	2.851(4)		*M*3	3.172(2) (2 ×)			
						*M*7	*As*2	2.746(2) (2 ×)
*As*2	*M*1	2.637(3) (2 ×)	*M*3	*As*1	2.730(2) (2 ×)		*As*3	2.834(3) (2 ×)
	*M*5	2.710(4)		*As*2	2.795(3) (2 ×)		*M*1	3.011(2) (2 ×)
	*M*7	2.746(2) (2 ×)		*M*4	3.095(2) (2 ×)		*As*2	3.106(4)
	*M*4	2.765(4)		*M*5	3.162(2) (2 ×)		*M*5	3.188(2) (2 ×)
	*M*3	2.795(3) (2 ×)		*M*2	3.172(2) (2 ×)			
	*M*7	3.106(4)						
			*M*4	*As*1	2.619(3) (2 ×)			
*As*3	*M*2	2.622(3) (2 ×)		*As*2	2.765(4)			
	*M*1	2.672(4)		*M*1	2.839(3) (2 ×)			
	*M*6	2.760(2) (2 ×)		*M*5	2.873(3) (2 ×)			
	*M*5	2.770(4)		*M*3	3.095(2) (2 ×)			
	*M*7	2.834(3) (2 ×)		*M*2	3.158(3)			
	M6	3.102(3)						
			*M*5	*As*2	2.710(4)			
*M*1	*As*2	2.637(3) (2 ×)		*As*3	2.770(4)			
	*As*3	2.672(4)		*As*1	2.851(4)			
	*As*1	2.749(4)		*M*2	2.866(2) (2 ×)			
	*M*4	2.839(3) (2 ×)		*M*4	2.873(3) (2 ×)			
	*M*7	3.011(2) (2 ×)		*M*3	3.162(2) (2 ×)			
	*M*6	3.235(2) (2 ×)		*M*7	3.188(2) (2 ×)			

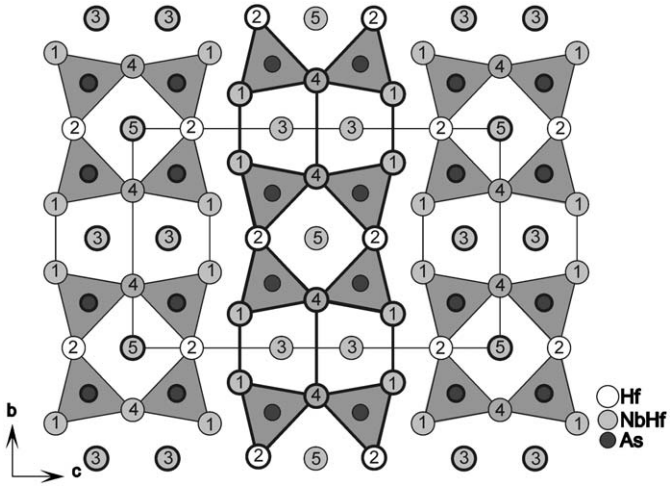

Fig. 3. The crystal structure of $Hf_{7.2}Nb_{3.8}As_4$ (Space group: *Immm*, Pearson symbol: *oI*30) projected in [100] direction. Grey triangles: trigonal prismatic units centred by As. *M*-sites are numbered according to the site designation given in Table 2. The *M*-atoms at $x=0$ are connected with thick lines, at $x=0.5$ with thin lines.

coordination numbers of 14 and 17, respectively. Two of the five metal positions, *M*3 and *M*5, are situated in the centre of more or less distorted metal cubes and thus represent distorted bcc fragments. A bcc-like coordination is also found in *M*1 for which the distorted cube is formed from 2 *As*- and 6 *M*-positions. *M*2 and *M*4 (again these are the nodes connecting the trigonal prismatic units) are coordinated by capped pentagonal prisms (CN=17). The coordination polyhedra of all metal positions are shown in Fig. 4. Selected interatomic distances for $Hf_{7.2}Nb_{3.8}As_4$ are listed in Table 6.

Similar to $Hf_{3\pm\delta}Nb_{4\pm\delta}As_3$, the observed site occupations at the different metal sites can be well understood based on the differences in coordination. Hf preferably enters the higher coordinated positions *M*2 and *M*4 (occupation numbers 1.00 and 0.97, respectively) while the other three positions show relative enrichment of Nb. These site occupations are in good agreement with the results for $Zr_{6.45}Nb_{4.55}P_4$ showing Zr at the pentagonal prismatic sites and mixtures of Nb and Zr at the three other positions [19]. The analysis of site volumes listed in Table 4 presents that these are not in full agreement with the observed site occupations. While, in agreement with expectations, *M*1 has the smallest volume and the highest Nb occupation number, *M*3 and *M*5 show the largest volumes but still around 0.3 Nb-occupation. For the compound $Zr_{6.45}Nb_{4.55}P_4$, Marking and Franzen [19] analysed the bonding situation based on Pauling bond order calculations [21] and found that the experimentally observed site occupations agreed well with the total Pauling bond orders calculated using linearly averaged Pauling radii for the mixed occupied sites. According to these results, the fraction of Zr and Nb at the different metal sites is primarily determined by the different numbers of valence electrons of Zr (4 electrons) and Nb (5 electrons) as the calculated total Pauling bond orders agreed well with the site valence of the metal positions (averaged according to the mixed site occupation). A similar approach was also tested for $Hf_{7.2}Nb_{3.8}As_4$ and the respective calculated Pauling bond orders are given in Table 4. As can be seen, the total Pauling bond orders (calculated as the sum of all bond orders of the *M*–*M* and *M*–*As* contacts of the coordination polyhedron) do not agree well with the observed site occupations except for *M*1 which has the highest total PBO corresponding to highest fraction of Nb present in this position. If only the *M*–*M* contacts are considered, the sum of PBOs agrees much better with the experimentally observed site fractions, e.g. the most Hf-rich positions (*M*2 and *M*4) are also those with the lowest sum of *M*–*M* PBOs. This is consistent with the fact that Nb has a larger enthalpy of sublimation [22] and thus a higher ability to form strong metal–metal bonds. In summary it may be stated that the site occupations can only be understood by considering size as well as bonding arguments.

3.3. Homologous series $M_{k+2l+m}X_{2m}$

The two new ternary compounds described here belong to a large group of metal-rich pnictides and chalcogenides that share common structural characteristics. As already mentioned in the introduction, the non-metals in these structures are coordinated in the form of tri-capped trigonal prisms and parts of the metal atoms are found in a bcc-like coordination environment. The occurrence of bcc-like units is strongly correlated with the stoichiometry, as a higher metal content usually yields the condensation of isolated bcc fragments to more extended clusters. Structures of this type have one short structural axis perpendicular to a mirror plane which contains all atoms. Typical examples for binary structure types belonging to this group are Ti_8S_3 (*C*2/*m*) [23], Nb_8P_5 (*Pbam*) [24], $Nb_{21}S_8$ (*I*4/*m*) [25] and Nb_5As_3 (*Pnma*) [26]. In addition to the binary structure types, several new ternary compounds with unique structure types and stabilized by differential fractional site occupation have been synthesized in recent years. This includes, among others, $Hf_{5.08}Mo_{0.92}P_3$ (*Pnma*) [27], $Nb_{6.74}Ta_{5.26}S_4$ (*Pnma*) [28] and $Zr_{6.45}Nb_{4.55}P_4$ (*Immm*) [19].

Three new compounds synthesized in the Hf–Nb–As system, $Hf_{1.5+\delta}Nb_{1.5-\delta}As$ (*Pnma*) [12], $Hf_{3\pm\delta}Nb_{4\pm\delta}As_3$ and $Hf_{7.2}Nb_{3.8}As_4$, clearly belong to this group of structures. However, they show one additional feature which is not found in any of the previously mentioned compounds. While the trigonal prismatic units are usually orientated in different directions, with the basal plane of the prisma situated either within or perpendicular to the special

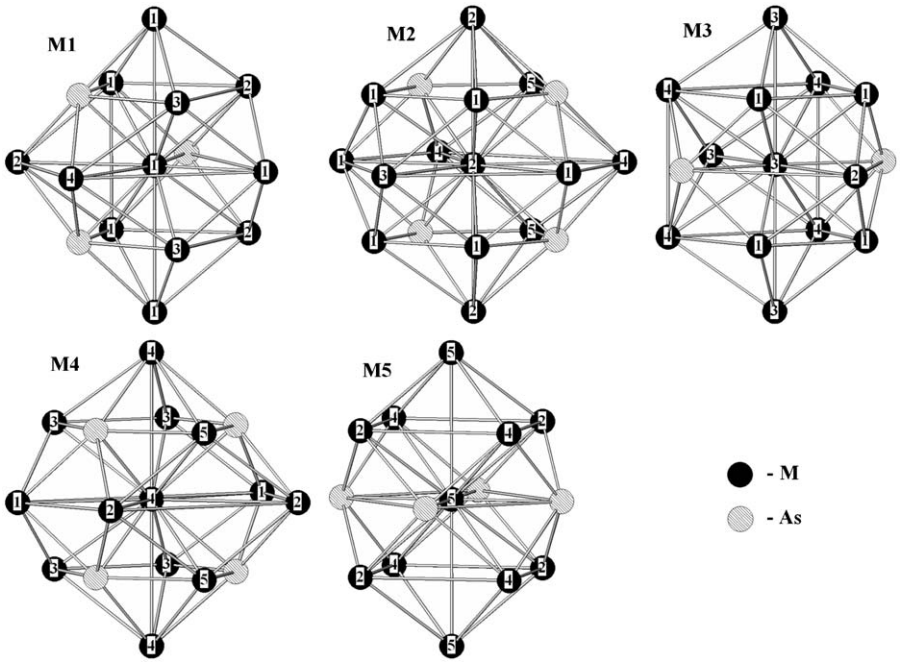

Fig. 4. Coordination polyhedra of the five independent metal sites in $Hf_{7.2}Nb_{3.8}As_4$. The numbers correspond to the numbering of sites in Table 2.

Table 6
Selected interatomic distances in $Hf_{7.2}Nb_{3.8}As_4$.

Bond		Distance (Å)	Bond		Distance (Å)	Bond		Distance (Å)
As	*M*1	2.655(1) (2 ×)	*M*2	*As*	2.749(1) (4 ×)	*M*4	*As*	2.731(1) (4 ×)
	*M*4	2.731(1) (2 ×)		*M*5	3.141(1) (2 ×)		*M*3	3.167(1) (4 ×)
	*M*2	2.749(1) (2 ×)		*M*1	3.142(1) (4 ×)		*M*5	3.247(1) (2 ×)
	*M*5	2.765(1)		*M*1	3.402(1) (2 ×)		*M*1	3.423(1) (2 ×)
	*M*1	2.795(2)						
	*M*3	2.852(1)	*M*3	*As*	2.852(1) (2 ×)	*M*5	*As*	2.765(1) (4 ×)
				*M*1	2.958(1) (4 ×)		*M*2	3.141(1) (4 ×)
*M*1	*As*	2.655(1) (2 ×)		*M*3	3.108(2)		*M*4	3.247(1) (4 ×)
	As	2.795(2)		*M*4	3.167(1) (4 ×)			
	*M*1	2.865(1) (2 ×)						
	*M*3	2.958(1) (2 ×)						
	*M*1	2.998(2)						
	*M*2	3.142(1) (2 ×)						
	*M*2	3.402(1)						
	*M*4	3.423(1)						

mirror plane, the three compounds in the Hf–Nb–As system have all their trigonal prisms orientated with their basal plane within the mirror plane. As a consequence, the interconnection among the building blocks is especially simple. All trigonal prismatic units are stacked to columns along the short axis. These columns may share common edges with neighbouring trigonal prismatic columns and they may share side faces with adjacent bcc fragments. Bcc fragments as well as trigonal prisms can have their basal planes situated in one of the two mirror planes within the unit cell, i.e. either at $y=1/4$ or 3/4 in *Pnma* and either at $x=0$ or 1/2 in *Immm*. Consequently the structures contain larger subunits formed from condensed trigonal prisms and bcc fragments that are shifted for a half translation period. These larger subunits are interconnected by a third type of building block that resembles distorted fragments of the hcp (Mg-type) structure.

A graphical representation of the structures of $Hf_{1.5+\delta}Nb_{1.5-\delta}As$ (own structure type), $Hf_{3\pm\delta}Nb_{4\pm\delta}As_3$ ($M_3Pd_4P_3$-type) and $Hf_{7.2}Nb_{3.8}As_4$ ($Zr_{6.45}Nb_{4.55}P_4$-type) emphasizing the three different building blocks is given in Fig. 5. All structures are projected along their short axis and the different planes are distinguished by dashed and straight lines, respectively. The structural motifs found in the different structures are quite different. The most metal-poor compound, $Hf_{3\pm\delta}Nb_{4\pm\delta}As_3$ (70% metal atoms), shows isolated bcc fragments (centred on *M*5) which are condensed with three trigonal prisms forming lager subunits of more or less triangular shape. Subunits of the same set (basal plane at $y=1/4$ or 3/4) share common edges via trigonal prisms and subunits of different sets are interconnected by Mg-type fragments forming infinite winding chains. The compound $Hf_{7.2}Nb_{3.8}As_4$ (73.3% metal atoms) shows isolated bcc fragments (centred on *M*5) and pairs of bcc fragments sharing a common face (centred on *M*3). These bcc fragments are condensed with trigonal prisms forming infinite slabs in *b*-direction. Slabs of different sets (basal plane at $x=0$ or 1/2) are again interconnected by Mg-type fragments forming infinite chains. In the most metal-rich compound of this series, $Hf_{1.5+\delta}Nb_{1.5-\delta}As$ (75%

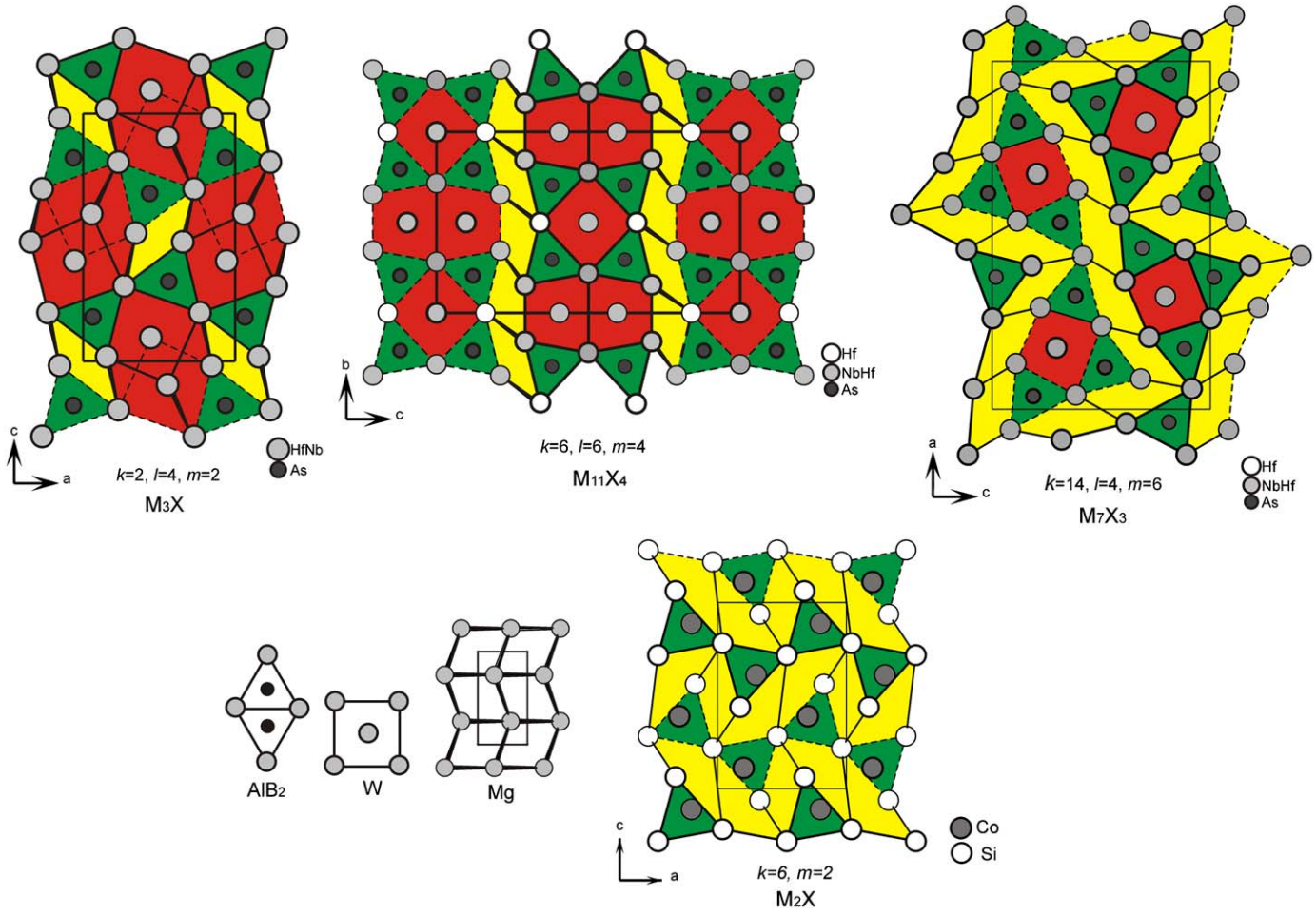

Fig. 5. A comparison of the structures of $Hf_{1.5+\delta}Nb_{1.5-\delta}As$ (left), $Hf_{7.2}Nb_{3.8}As_4$ (centre) and $Hf_{3\pm\delta}Nb_{4\pm\delta}As_3$ (right) represented as combination of Mg-type (yellow), W-type (red) and AlB_2-type (green) building blocks. The structures are projected on their short axis. The atoms in the bottom and top planes are connected by straight and dashed lines, respectively. The structure of Co_2Si is given for comparison.

metal atoms), bcc units at $y=1/4$ and 3/4 are interpenetrating to form condensed columns in b-direction. In fact, the motif of interpenetrating bcc fragments is quite common in metal rich compounds and is found, e.g. in the structures of Ti_8S_3 ($C2/m$) [23] and $Nb_{21}S_8$ ($I4/m$) [25]. The bcc units are condensed with trigonal prisms of the same set via their side faces and the Mg-type units interconnecting the different sets are isolated.

To our knowledge, the three structure types discussed here are the only ones of this series that have all their trigonal prisms aligned along the short axis, but it is clear that many other structures combining these building blocks in an aligned way are possible. $Hf_{1.5+\delta}Nb_{1.5-\delta}As$, $Hf_{3\pm\delta}Nb_{4\pm\delta}As_3$ and $Hf_{7.2}Nb_{3.8}As_4$ are members of a homologous series that can be described by the same general formula. Using the index k for the number of Mg-type fragments, the index l for the number of W-type fragments and the index m for half of the number of the trigonal-prisms (AlB_2-type fragments), the general formula can be given as $M_{k+2l+m}X_{2m}$. In case of $Hf_{1.5+\delta}Nb_{1.5-\delta}As$ ($k=2$, $l=4$, $m=2$) the general formula is $M_{12}X_4$, i.e. M_3X with $Z=4$ corresponding to content of the unit cell. For $Hf_{7.2}Nb_{3.8}As_4$ ($k=6$, $l=6$, $m=4$) the general formula is $M_{22}X_8$ ($M_{11}X_4$ with $Z=2$) and for $Hf_{3\pm\delta}Nb_{4\pm\delta}As_3$ ($k=14$, $l=4$ and $m=6$) we calculate $M_{28}X_{12}$ (M_7X_3 with $Z=4$). Obviously the ratios of k, l and m depend on the different ways to condense W-type and AlB_2-type fragments to larger units. As there are quite different ways to form these units, a systematic analysis of resulting stoichiometries appears to be a complex task. However, it may be stated that the number of W-type fragments is directly related to the amount of metal found in the structure. This means that metal-rich compounds contain a larger number of W-type building blocks which then condense to larger units, either by sharing common faces or by interpenetration. In this light, it is possible to define a metal-poor limiting member of the structural series with no W-type building blocks present. In fact, the well-known Co_2Si type structure (*Pnma*, *oP*12) with 66.7% metal may be identified as limiting member as shown in Fig. 5. Remarkably, a ternary arsenide of this structure type was reported in the Hf–V–As system [29]. In case of the Co_2Si-type, the indices $k=6$, $l=0$ and $m=2$ again lead to the correct representation of the general formula M_8X_4, i.e. M_2X with $Z=4$.

Acknowledgment

Financial support from the Austrian Science Foundation (FWF) under the Project number P16946-N11 is gratefully acknowledged.

Appendix A. Supplementary material

Supplementary data associated with this article can be found in the online version at doi:10.1016/j.jssc.2009.12.028.

References

[1] H.F. Franzen, M. Köckerling, Prog. Solid State Chem. 23 (1995) 265–289.
[2] H. Kleinke, Trends Inorg. Chem. 7 (2001) 135–149.
[3] C.-S. Lee, E. Dashjav, H. Kleinke, J. Alloys Compd. 338 (2002) 60–68.
[4] A. Assoud, S. Derakhshan, K.M. Kleinke, H. Kleinke, J. Solid State Chem. 179 (2006) 464–469.
[5] K.W. Richter, H. Flandorfer, H.F. Franzen, J. Solid State Chem. 167 (2002) 517–524.
[6] K.W. Richter, H.F. Franzen, J. Solid State Chem. 150 (2000) 347–355.
[7] K.W. Richter, R. Picha, H. Ipser, H.F. Franzen, Solid State Sci. 5 (2003) 653–662.
[8] N. Ponweiser, P. Warczok, C.L. Lengauer, K.W. Richter, Solid State Sci. 11 (2009) 395–401.
[9] M.C.J. Marker, H.S. Effenberger, K.W. Richter, Solid State Sci. 11 (2009) 1475–1483.
[10] K.W. Richter, Monatsh. Chem. 136 (2005) 1885–1897.
[11] P. Warczok, F. Mittendorfer, G. Kresse, A. Kroupa, H. Ipser, K.W. Richter, Solid State Sci. 9 (2007) 159–165.
[12] P. Warczok, I. Chumak, K.W. Richter, J. Solid State Chem. 182 (2009) 896–904.
[13] TOPAS, Bruker AXS Inc., Karlsruhe, Germany, 1999.
[14] Z. Otwinowski, D. Borek, W. Majewski, W. Minor, Acta Crystallogr. A 59 (2003) 228–234.
[15] G.M. Sheldrick, SHELX-97, University of Göttingen, 1997.
[16] J. Emsley, The Elements, Clarendon Press, Oxford, 1989.
[17] M. Wang, R. McDonald, A. Mar, Inorg. Chem. 39 (2000) 4936–4941.
[18] E. Koch, W. Fischer, Z. Kristallogr. 211 (1996) 251–253.
[19] G.A. Marking, H.F. Franzen, Chem. Mater. 5 (1993) 678–680.
[20] L.M. Gelato, E. Parthe, J. Appl. Crystallogr. 20 (1987) 139–143.
[21] L. Pauling, The Nature of the Chemical Bond, third ed., Cornell University Press, Itaca, NY, 1948.
[22] R. Hultgren, P.D. Desai, D.T. Hawkins, M. Gleiser, K. Kelley, D.D. Wagman, Selected Values of the Thermodynamic Properties of the Elements, ASM, Ohio, 1973.
[23] J.P. Owens, H.F. Franzen, Acta Crystallogr. Sect. B 30 (1974) 427–430.
[24] S. Anugal, C. Pontchour, S. Rundqvist, Acta Chem. Scand. (1947–1973) 27 (1973) 26–34.
[25] H.F. Franzen, T.A. Beineke, B.R. Conrad, Acta Crystallogr. Sect. B 24 (1968) 412–416.
[26] S. Laohavanich, S. Thanomkul, S. Pramatus, Acta Crystallogr. B 37 (1981) 227–228.
[27] J. Cheng, H.F. Franzen, J. Solid State Chem. 121 (1996) 362–371.
[28] X. Yao, H.F. Franzen, Z. Anorg. Allg. Chem. 598–599 (1991) 353–362.
[29] S. Derakhshan, E. Dashjav, H. Kleinke, Eur. J. Inorg. Chem. (2004) 1183–1189.